JOURNAL OF MATERIALS SCIENCE **34** (1999) 5089–5097

The effect of extrusion parameters on the fretting wear resistance of Al-based composites produced via powder metallurgy

J. ZHOU, A. T. DRUŻDŻEL*, J. DUSZCZYK
Laboratory for Materials Science, Delft University of Technology, Rotterdamseweg 137, 2628 AL Delft, The Netherlands

The work reported in this paper is aimed at establishing the relationship between processing and the wear resistance of the metal matrix composites (MMCs) based on a novel alloy, Al-20Si-5Fe-3Cu-1Mg. The MMCs were processed via a commercially viable powder metallurgy (PM) route, i.e. through mixing the atomized matrix alloy powder with 10 vol % SiC or Al_2O_3 particles, cold isostatic pressing, degassing and hot extrusion. It has been found that the extrusion window of the MMCs is greatly narrowed due to their increased deformation resistance on one hand and incipient melting of their matrix on the other. For a sound MMC extrudate, a reduction ratio over a critical value must be applied. However, a further rise of this ratio leads to deterioration of local interfacial cohesion between the ceramic phase and the matrix dispersed with a high volume fraction of silicon crystals and intermetallic dispersoids, thus degrading the MMCs in tensile properties. Furthermore, fretting wear tests at room and elevated temperatures and with dry and wet contacts show that the MMCs extruded at a higher reduction ratio has a higher mass loss and an increased friction coefficient. The work points to the direction of further research, i.e. on MMCs containing spherical reinforcement instead of commonly used angular particles.

1. Introduction

Since the 1980s, various advanced materials have emerged partly as a result of the strong need of material users to fulfil the requirements for environmental protection and energy efficiency. The advanced materials are defined as those with enhanced properties and of improved quality. The commercially viable advanced materials are those that can be produced relatively cheaply by using environment-friendly techniques. The materials (MMCs) developed and characterized in the present work fall into this category. They were expected to have the following characteristics in order to meet the requirements of the aerospace, aircraft, automobile and electronic industries:

- high wear resistance,
- low thermal expansion coefficient,
- low weight,
- enhanced tensile strength at elevated temperatures,
- reasonable price.

In recent years, the tendency of shifting the uses of the advanced materials from the defence and aerospace industries to civil ones becomes more and more notable, especially to the automotive industry. Development of high-performance vehicles requires new materials to be lighter, stiffer, stronger, and more temperature and wear resistant than today's counterparts. For example, the operational temperature in combustion engines tends to increase in the near future so as to permit a reduction in the emissions of exhaust gases, plus an increase in fuel efficiency. For such an application, MMCs must be based on thermally stable matrix alloys, although the reinforcing phase can enhance their thermal resistance to some extent.

The majority of MMCs based on conventional aluminium alloys do not fully satisfy this desire, largely due to structural coarsening with rising temperature. High-strength Al-Fe alloys produced by means of rapid-solidification techniques contain thermally stable intermetallic dispersoids. However, they are unlikely to meet the requirements in applications where components slide and rub against one another with tight tolerances, such as the piston-piston ring assembly in a conventional combustion engine, because of their high thermal expansion coefficients. Conventional ingot-cast Al-Si alloys have relatively low thermal expansion coefficients, but they suffer from alloying restrictions, phase inhomogeneity and brittleness.

In an effort to search for new piston materials, the Al-20Si-5Fe-3Cu-1Mg alloy has been designed and manufactured from rapidly solidified powder. The alloy exhibits encouraging properties: being strong at room

* *Present address*: International Tobacco Machinery Poland, Ltd., ul. Warsztatowa 19A, 26-600 Radom, Poland.

temperature, stiff, dimensionally stable and wear resistant [1]. The inclusion of 5 wt% iron in the alloy contributes toward these properties, particularly hot strength [2–4]. A further addition of 10 vol% SiC or Al_2O_3 particles to the alloy results in a significant enhancement in its wear resistance [1, 5, 6]. In selecting the ceramics to reinforce the alloy, the following criteria have been taken into consideration:

- low density,
- low thermal expansion coefficient,
- high strength and elastic modulus,
- low cost and commercial availability.

In the present work, an attempt was made to correlate some important process parameters used in the industrial manufacturing of the Al-20Si-5Fe-3Cu-1Mg based composites with their wear resistance. Within the industrial conditions, processing simplicity was a major concern. At the same time, it was also desired to make use of newly developed industrially applicable manufacturing technologies such as powder metallurgy (PM) that offers a significant potential of energy savings [7].

Once the commercially available raw materials, i.e. the matrix alloy as well as SiC and Al_2O_3 particles were chosen, they were subjected to mixing, cold isostatic pressing, degassing and hot extrusion. The process parameters (including temperature, strain and strain rate) used at the last step of processing, i.e. hot extrusion, were considered most influential on the mechanical properties and wear resistance of the MMCs. This is because only at this stage of processing were the basic properties of the MMCs as engineering materials developed.

In this paper, the extrudability of the MMCs is discussed with respect to temperature, reduction ratio and extrusion speed. As in any commercial production, speed is desired to be as high as possible, and as temperature was restricted by the phase constitution of the matrix alloy and the high stiffness of the MMCs, reduction ratio was left as the only variable. Therefore, in this paper, the influence of reduction ratio on the tensile properties and fretting wear resistance of the MMCs is mostly discussed.

2. Material processing and tensile property evaluation

The Al-20Si-5Fe-3Cu-1Mg matrix alloy was designed to take advantage of the alloying possibilities provided by atomization involving rapid solidification to prevent segregation from occurring. It should be noted that this matrix alloy cannot be produced by conventional foundry techniques, because it contains a high volume fraction of silicon crystals and fine intermetallic compounds (Al-Si-Fe).

The matrix powder used was supplied by Showa Denko K. K., Japan. It was atomized at a mean cooling rate of 10^4–10^6 $K \cdot s^{-1}$. The composition of the matrix alloy powder is given in Table I, and its relevant technical data are presented in Table II.

SiC in the form of powder used to reinforce the matrix alloy was supplied by Lonza, Germany. It had a size span of 5–50 μm and a median size of 23 μm. It was of highly irregular shape and with sharp edges. Al_2O_3 powder supplied by Cerac, USA, had a wider size span of 1.2–118 μm and a similar median size (24 μm). It had also an irregular shape but in comparison with the SiC powder it was more flake-like.

TABLE I Composition of the matrix alloy determined by atomic absorption spectrophotometry

Element	Si	Fe	Cu	Mg	Al
Wt%	19.2	5.17	3.24	1.18	Balance

TABLE II Technical data of the Al-based matrix alloy powder

Oxygen content	0.20%
Mass median size	64 μm
Density	2790 kg/m^3
Specific surface area	0.16 m^2/g

Among a variety of possible PM processing routes that can be followed to produce MMCs [1], the following procedure was chosen:

- mixing,
- cold isostatic pressing (CIPing),
- degassing combined with preheating for extrusion and assisted by flushing with nitrogen,
- hot extrusion or hot compaction.

First, the matrix powder was mixed with the ceramic powder (SiC or Al_2O_3) for 30 min using a 1213 HP turbula mixer. The mixtures were then subjected to CIPing. Prior to CIPing, a flexible rubber mould was filled with the mixture. During CIPing, the mould was pressurized isostatically by means of oil. Over a range of CIPing pressure from 250 to 400 MPa, green compacts were all sound enough for handling with care, but a relatively high pressure resulted in too much deformation of the matrix and formation of disconnected pores, which would lead to difficulties with degassing of green compacts. CIPing was finally optimized at a pressure of 300 MPa, which resulted in green compacts with a relative density of 74%.

The next operation, degassing, is generally regarded as an inevitable step in processing aluminium alloy powders. Powders have a large specific surface area, corresponding to a large amount of physically and chemically adsorbed moisture. During processing and service at elevated temperatures, the moisture would be converted into hydrogen to deteriorate the mechanical properties and surface appearance of the consolidated material. For effective degassing, powder is usually precompacted in a can, followed by hermetic sealing. After degassing, the canning material has to be removed from the consolidated material.

In the present experiments, in order to simplify the procedure and to make the whole processing cheaper, degassing was combined with preheating before extrusion and assisted by flushing with nitrogen. The degassing temperature was selected to be the same as the temperature of extrusion, varying between 400 and 500 °C (most frequently 450 °C).

It is well known that when aluminium is exposed to an atmosphere containing oxygen and moisture, due to

its high affinity to oxygen, oxidation unavoidably takes place, as shown below.

$$4Al + 3O_2 \rightarrow 2Al_2O_3$$

$$2Al + 3H_2O \rightarrow Al_2O_3 + 3H_2$$

During and after an aluminium alloy powder is atomized, these reactions take place and, as a result, an aluminium oxide layer is formed on the powder particle surface. This surface layer tends to adsorb moisture and form hydroxides:

$$Al_2O_3 + H_2O \rightarrow 2AlOOH$$

$$AlOOH + H_2O \rightarrow Al(OH)_3$$

Both hydration and dehydration processes depend on temperature and the partial pressure of water, which provides guidance to the selection of proper degassing conditions. Thus, a commonly used degassing condition is the combination of an elevated temperature and a high vacuum environment. Under the condition where the dew point is low and so is the oxygen partial pressure, adsorbed compounds will efficiently evacuate and further oxidation can be effectively minimized.

Degassing in an inert gas atmosphere, with gas flushing and at elevated temperatures may not be as effective as in vacuum, due to residual oxygen remaining inside the pores between powder particles. However, using an inert gas atmosphere instead of high vacuum remarkably simplifies the procedure and reduces the requirements for equipment, thus making the whole operation less expensive. Moreover, it has been found [8] that degassing in an inert gas atmosphere improves the resistance to re-hydration and re-adsorption of moisture during post-degassing processing or storage, in comparison with degassing in vacuum. Considering the above, degassing at elevated temperatures, in a nitrogen atmosphere and with gas flushing was applied during the processing of the MMCs in the present work.

Once nitrogen was chosen as the protective atmosphere for degassing, temperature and time remained the variables affecting the extent of the evolutions of gaseous compounds. When an aluminium alloy powder is exposed to elevated temperatures, the following reactions may take place:

$$Al_2O_3 \cdot 3H_2O \rightarrow Al_2O_3 \cdot H_2O + 2H_2O \uparrow$$

$$Al_2O_3 \cdot H_2O \rightarrow Al_2O_3 + H_2O \uparrow$$

$$2Al + 4H_2O \rightarrow Al_2O_3 \cdot H_2O + 3H_2 \uparrow$$

$$2Al + 6H_2O \rightarrow Al_2O_3 \cdot 3H_2O + 3H_2 \uparrow$$

The above reactions imply that the effectiveness of degassing to remove water vapour and hydrogen is governed by temperature, the partial pressure of water vapour and free aluminium available. It should be noted that what really affects gas evolution is not the pressure level, but the partial pressure that should be lower than that of the equilibrium, in order to allow surface reactions to occur. Considering this, and after a series of experiments as well as a fundamental work on vacuum degassing, the following condition was chosen:

- A vacuum atmosphere was replaced by nitrogen flushing to purge the evolved compounds.
- Billets were heated up to an extrusion temperature in the range of 400–500 °C for 100 min with nitrogen flushing.
- A soak at the degassing temperature for 40 min in a preheating furnace was given in order to allow gas evolutions to proceed.

Since the materials were not intended to be heat treated after hot extrusion, there was little chance for blistering to occur, as caused by further gas evolutions (most dangerously, evolution of hydrogen) at temperatures above the degassing temperature. Therefore, with the present degassing condition, the service temperature of the MMCs should not exceed the degassing temperature that is the same as the billet preheating temperature for extrusion.

As the next step, hot extrusion was performed with an industrial extrusion press to consolidate the green compacts. A degassed billet was transported from the preheating furnace to the container of the press and then extruded with a flat die. Prior to extrusion, the die was heated to the same temperature as the billet, i.e. between 400 and 500 °C. Reduction ratios varied from 5 : 1 to 40 : 1, yielding extrudates with diameters of 23.5 to 8.5 mm, respectively. Ram speed varied from 4.1 to 25 mm/s, which was self-adjusted, according to the temperature of the product extruded at full press power capacity. The variables of extrusion were thus temperature and reduction ratio.

Different values of reduction ratio and billet temperature were used to examine the effect of strain, strain rate and temperature on the quality of composite structure and extrudability (which is usually defined as the maximum exit speed that can be applied without tearing). Some of the extrusion conditions and results are presented in Table III.

Finally, the extrudates were subjected to tensile tests at room temperature, in the direction of extrusion, to determine ultimate tensile strength and elongation to fracture, using a computer-controlled Instron tensile machine. Cylindrical specimens had a gauge length of 30 mm and a gauge diameter of 4 mm. An extensometer clipping on the gauge section of the specimen was used to determine strain. A crosshead speed of 0.35 mm/s was selected, corresponding to an initial strain rate of 1.9×10^{-4} s^{-1}.

TABLE III Conditions and results of hot extrusion

	Exit speed (m/min)	Ram speed (mm/s)	Remark on quality
At reduction ratio 5 : 1			
Matrix (M)	2.75–2.9	9.1–9.7	Shiny
Matrix + 10 vol % SiC	3.5	11.7	Shiny
Matrix + 10 vol % Al_2O_3	3.5–4.0	11.7–13.3	Shiny
At reduction ratio 20 : 1			
Matrix (M)	25–30	21–25	Surface
Matrix + 10 vol % SiC	25–30	21–25	tearing
Matrix + 10 vol % Al_2O_3	25–30	21–25	after 40 mm

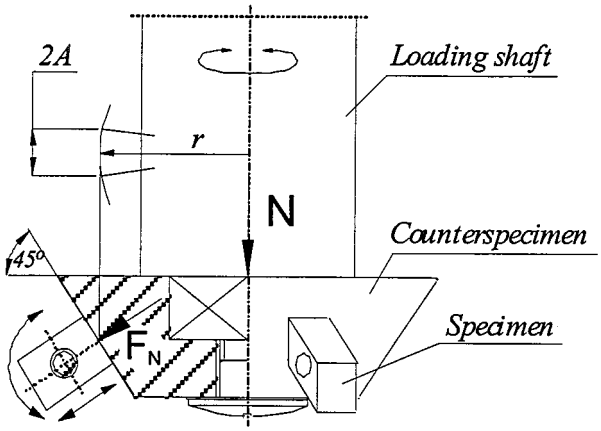

Figure 1 Configuration of specimens and counterspecimen in the fretting wear testing (the friction direction of the specimens being perpendicular to the extrusion direction).

3. Tribological tests

The wear resistance of the materials extruded at 5 : 1 and 20 : 1 was assessed by means of a fretting wear tester. It was designed to produce reciprocating relative displacement, representing in a simplified manner a practical working situation where many contacting components are placed, such as the piston-piston ring assembly in a combustion engine. A schematic drawing of the specimen assembly is shown in Fig. 1.

The specimen configuration of the fretting wear tester consisted of a conically shaped counterspecimen, made of grey cast iron (resembling the material for piston ring), and three rectangular PM specimens (resembling the potential materials for piston) which were placed underneath the counterspecimen. The specimens were mounted in specimen holders and distributed evenly along the lateral surface of the cone, i.e. at an interval of 120°. The mating surfaces of the specimens against the counterspecimen were perpendicular to the extrusion direction.

The specimen holders allowed free movement of the specimens in two directions, i.e. linear movement along the axis perpendicular to the lateral surface of the cone and, simultaneously, revolution of the specimen (around the axis perpendicular to the page), as schematically shown in Fig. 1. This configuration was chosen to secure optimal, permanent alignment between the lower specimens and the upper conical counterspecimen. Its advantage lies in the elimination of a detrimental stress distribution between mating surfaces, which may occur with inflexible assembling. During assembling, the attachment of the loading shaft to the cone was ensured by a screw joint of a tightly fitted square-shaped pin at the lower tip of the loading shaft and a mortise in the cone.

During the tests, the pneumatically loaded vertical shaft and the cast iron (CI) counterspecimen oscillated at a constant frequency and an invariable amplitude, while the three lower specimens remained motionless in the specimen holder. Thus, the friction couple operated under the condition of oscillatory motion.

The initial contact between the specimens and the surface of the cone was line contact. Thus, the tests started under the condition of a high initial contact pressure, as determined by elastic deformation of the mating surfaces. Although the initial line contact led to high initial Hertzian pressures, p_{Hi}, upon running-in, the contact pressure rapidly diminished. This was due to wear, leading to mass loss of the mating surfaces and consequently to adaptation of the contact surfaces of the specimens to the radius of the cone surface. Normal forces of 37 and 72 N were applied to the counterspecimen, which yielded initial line contact pressures of 71 and 100 MPa, respectively. However, with wear process proceeding, the high values of initial line-contact pressure decreased at full conformity to 1.5 and 3.0 MPa, respectively. The counterspecimen oscillated against the specimens at an amplitude of 385 μm and a frequency of 33 s^{-1}. Mass loss was measured at regular intervals until the curve of the mass loss versus the number of oscillations (cycles) was stabilized. At least 10×10^6 cycles were run, corresponding to a total sliding distance of 15360 m covered by each specimen. The testing conditions are summarized in Table IV [9].

TABLE IV Conditions applied during the wear tests

Parameter	Value
Amplitude, A (μm)	385
Ambient temperature, T (°C)	22 and 200
Frequency, f (s^{-1})	33
Normal force, F_N (N)	36 and 72
Initial-line (Hertzian) pressure, p_{Hi} (MPa)	71 and 100
Contact pressure at full conformity, p_c (MPa)	1.5 and 3.0

During the wear testing of the PM specimens (i.e. the matrix alloy and the MMCs), the following environments were used.

(1) Kerosene was used as the environment for the friction couple during the tests at room temperature. This testing environment was considered reference conditions. During the tests, the specimen assembly was completely submerged in a kerosene bath in order to protect the friction couple from severe oxidation and from humidity change. In such an environment, the behaviour of the materials could be studied without the influence of any lubricant and its various additives, i.e. under the conditions of extremely poor lubricity. In practice, because of stringent environmental regulations, there is a worldwide tendency toward limiting exhaust and smoke emissions from vehicles by using so-called reformulated fuels with reduced lubricity.

(2) A heat-resistant oil was employed as the environment for the wear tests at 200 °C in order to protect the mating surfaces from oxidation and to provide sufficient lubrication. This environment was of particular interest from the viewpoint of the potential applications of the materials in question, i.e. inside the combustion chamber of an internal combustion engine.

4. Results and discussion

4.1. Extrusion characteristics

Extrusion at 400 °C was impossible because the force required for breakthrough went beyond the power limit of the press used. At 500 °C , fine cracks appeared on the surfaces of the products extruded at different reduction

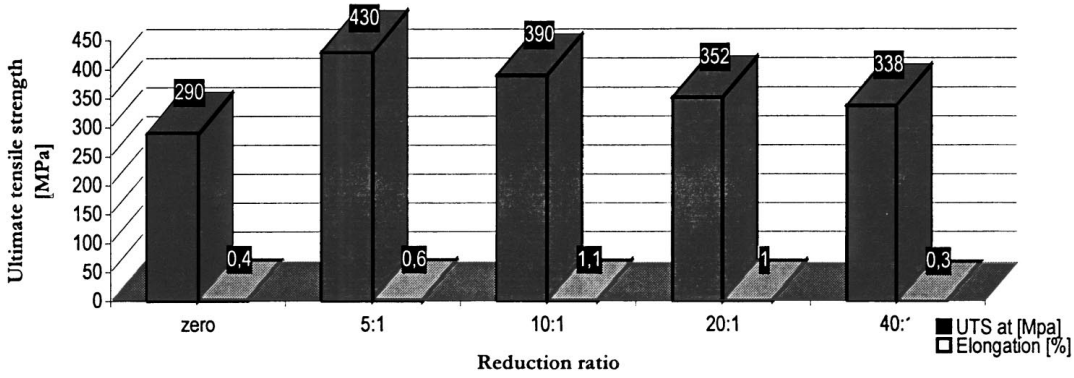

Figure 2 Room-temperature tensile properties of the composite containing 10 vol % SiC, extruded at different reduction ratios.

ratios, indicating that heating as a result of mechanical work and friction brought the temperature of the material above the incipient melting point of the matrix.

Differential scanning calorimetry of a similar composite shows that endothermic reactions start at about 507 °C, which correspond to the melting of the $Al_5Cu_2Mg_8Si_6$ and Al_7Cu_2Fe phases [10]. Thus, the occurrence of hot shortness and the power limit of the press restricted the extrusion temperature to about 450 °C .

However, at that temperature another defect at the surface of the extrudate, i.e. stick-slip tearing, was observed. This defect appeared occasionally, when the friction exerted on the MMC extrudate was so high that it exceeded the fracture stress of the matrix. In addition, because no lubrication was applied during extrusion, the surface quality of the extrudate solely relied on the material properties and extrusion conditions. Clearly, the interactions between the die material (AISI H13 hot-work tool steel) and the MMCs, the scrubbing action of the hard particles (Si-crystals and SiC or Al_2O_3) of a very high volume fraction in the MMCs on the die surface, together with their low hot ductility, favoured the occurrence of the defect. It appeared to be also related to the billet temperature, die temperature, reduction ratio and exit speed in a complex way. In most cases, it tended to occur after a certain length (volume) of the MMC material had been extruded. Probably, by that time, the transferred layer formed on the die surface became unstable and vulnerable to breakage due to local severe working conditions. When the reduction ratio was low and thus the extrudate was short, the defect was negligible or did not occur at all. However, when the reduction ratio was high and then the exit speed was proportionally high, the surface of the ending part of the extrudate became rough, while the beginning part was shiny. In the worst instance, i.e. when the die cooled down after a few extrusion runs, seizure occurred. Although the surface layer with the defect could be machined off, the problem as to how to ensure the surface quality of an extruded MMC based on a high-strength, low-ductility aluminium alloy and containing phases with low melting points remains to be solved. An industrially viable solution should neither complicate processing, such as canning billets or applying lubrication, nor sacrifice productivity by using a low extrusion speed.

4.2. Tensile properties

Fig. 2 shows the ultimate tensile strength (UTS) and elongation of the MMC containing 10% SiC at room temperature, as a function of reduction ratio applied during hot extrusion. The strength values are all higher than the strength of the composite based on a conventional Al-Si alloy (A356) and containing 10 vol % SiC (283 MPa) [11].

From Fig. 2, it can be seen that the tensile properties are indeed affected by extrusion ratio applied during extrusion. The low strength and elongation values at zero reduction ratio (namely hot compaction in the extrusion container with a blind die) can be attributed to weak bonding between the original powder particles (the matrix alloy and SiC particles). Fractographic study of the matrix alloy extruded at 2.5 : 1 shows that debonding between the original powder particles is responsible for the premature fracture of the material, which has undergone insufficient shear deformation to break up and redistribute the oxides at the original powder particle boundaries [12]. Therefore, a threshold of shear deformation, corresponding to a critical reduction ratio, is needed to obliterate the boundaries, which is generally agreed to be 5 : 1 [13]. However, at that reduction ratio, the percentage elongation of the composite is poor. This is probably caused by the oxides and the ceramic particles at the original powder particle boundaries, which are insufficiently redistributed during processing. For monolithic aluminium alloys, strength and elongation have been observed to increase with rising reduction ratio till approximately 10 : 1 and then stabilize or moderately increase, if there is no structural change affecting the trend. However, such a trend has not been observed for the present MMCs. At reduction ratios above 5 : 1, strength decreases with increasing reduction ratio (see Fig. 2).

Stress/strain curves showed that the material failed during the continuous, non-linear load increase, indicating that it was the brittle fracture of the materials, which could be caused by internal stresses and defects, that interrupted the development of normal elastic-plastic deformation in tensile testing.

4.3. Tribological tests at room temperature and in kerosene

Figs 3 and 4 give the data on the wear of the PM specimens extruded at 5 : 1 and 20 : 1 and then tested at

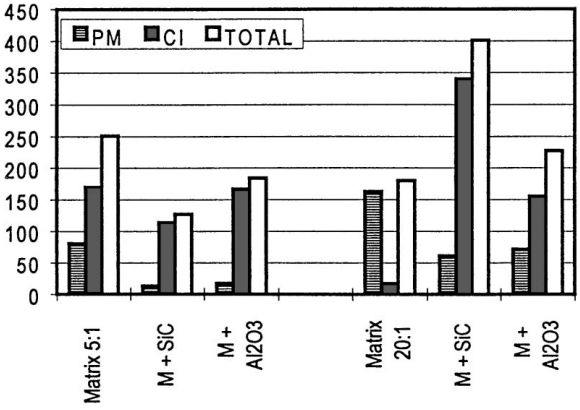

Figure 3 Volume losses per contact cycle $\Delta V/N_c$ (mm^3/cycle $\times$ 10^{-9}) of the PM specimens and grey cast iron (CI) counterspecimen under the reference conditions and at the load $F_N = 36$ N.

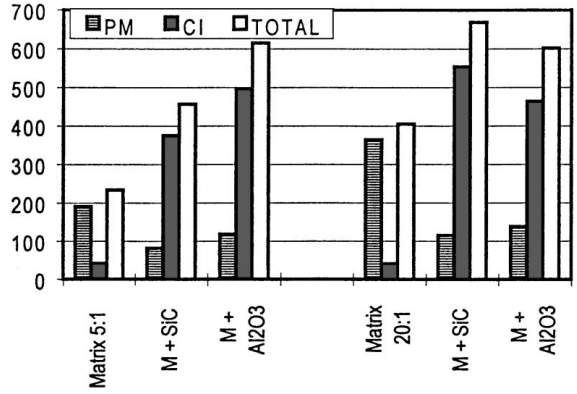

Figure 4 Volume losses per contact cycle $\Delta V/N_c$ (mm^3/cycle $\times$ 10^{-9}) of the PM specimens and grey cast iron (CI) counterspecimen under the reference conditions and at the load $F_N = 72$ N.

$F_N = 36$ and 72 N, respectively. Wear is expressed by the volume loss calculated per contact cycle, $\Delta V/N_c$ (mm^3/cycle $\times$ 10^{-9}). From the figures, the beneficial effect of the two types of ceramic reinforcement in the MMCs on the wear resistance is evident. The MMC with SiC addition exhibits the highest wear resistance at both of the loads applied. It can also be seen that the PM materials, i.e. both the matrix and the MMCs, extruded at a lower reduction ratio (5 : 1) yield less wear than those extruded at a higher reduction ratio (20 : 1). The influence of reduction ratio on wear resistance is apparent also at both the loads applied. SEM analysis of the wear-tested specimens revealed structural defects in the MMCs extruded at 20 : 1, i.e. decohesion around sharp edges of the reinforcing particles (see Fig. 5), as observed in the extruded materials [1, 9, 14].

Decohesion may have originated from manufacturing of the MMCs, when a pressure of 300 MPa was applied during CIPing and especially when severe shear deformation was exerted during extrusion. It may also have formed during machining; the interaction between a cutting edge and the ceramic reinforcement may have led to stress concentrations in the vicinities of the tips of angular particles. Therefore, the stress concentrations may be responsible for decohesion in the matrix/reinforcement interface and microcrack propagation in the matrix material. Considering that the same machining parameters were applied to all of

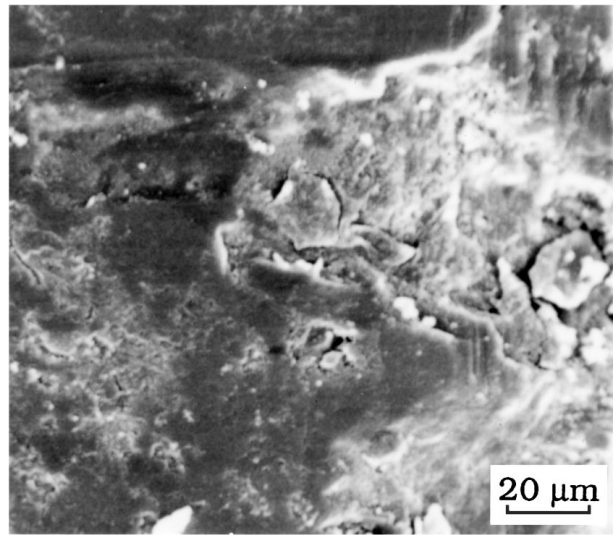

Figure 5 Topography of the composite containing 10 vol % SiC extruded at 20 : 1 and tested at room temperature, at the load of 36 N and in kerosene, after 0.5×10^6 cycles, showing decohesion around the sharp edges of the reinforcing particles.

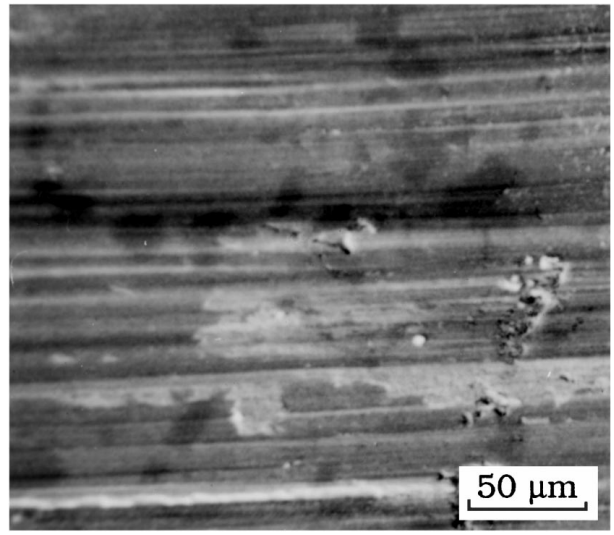

Figure 6 Topography of the composite containing 10 vol % SiC extruded at 5 : 1 and tested at room temperature, at the load of 36 N and in kerosene, after 18.5×10^6 cycles, showing non-uniformly distributed wear tracks.

the PM specimens, a lower reduction ratio (5 : 1), i.e. lower shear stresses generated during extrusion, yields a sound structure with less internal defect, which leads to better wear resistance.

Decohesion between the reinforcing particles and the matrix may contribute substantially to the wear of the MMCs. It is likely that reciprocating movement in the friction zone results in fatigue, thereby accelerating the development of the decohesion at the matrix/reinforcement interface. Finally, the hard particles are pulled out. When the hard ceramic particles with an angular shape are free to move in the friction zone, they accelerate the abrasion of both mating surfaces.

SEM analysis of the wear-tested MMCs extruded at 5 : 1 revealed scratches and grooves within wear paths, as shown in Fig. 6. No significant differences in the depth or shape of the scratches and grooves with respect

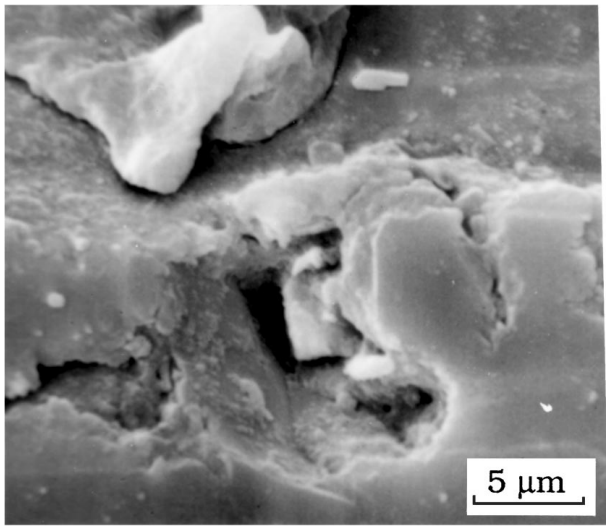

Figure 7 Topography of the composite containing 10 vol % SiC extruded at 20 : 1 and tested at room temperature, at the load of 36 N and in kerosene, after 0.5×10^6 cycles, showing voids around the SiC particles.

to the load applied were found for the materials extruded at 5 : 1. It implies mild wear, even after a long sliding distance up to 30×10^3 m. SEM analysis of the wear-tested material extruded at 20 : 1 however showed voids with faceted walls and microzones with a reduced density, as shown in Fig. 7. This structural imperfection may arise from a high volume fraction of hard Si-crystals and intermetallics in the matrix and more importantly from reinforcing particles, SiC or Al_2O_3. The hard ceramic particles and the dispersoids in the matrix are not deformable. Their presence may be in the form of micro-clusters, opposing further densification during extrusion. Therefore, this may result in the formation of undensified regions on a micro scale. In turn, they may act as a source of cracks during the fretting wear tests under the condition of oscillatory motion. As a result, increased removal of the material could be anticipated.

From a practical point of view, it is of great importance to consider the total volume loss of the whole friction couple (i.e. specimen plus counterspecimen), which will be directly related to the development of clearances or leakage. Therefore, the total volume losses of the friction couples are presented in Figs 3 and 4. It can be seen that when the applied load is low ($F_N = 36$ N), the ceramic reinforcement in the MMCs extruded at 5 : 1 brings down the total wear, while the same reinforcement in the MMCs extruded at 20 : 1 enhances the wear of the counterspecimen and thus the total wear although it decreases the wear of the MMC specimens. Clearly, it is associated with the angular morphology of the hard ceramic particles that are strongly abrasive to the cast-iron counterspecimen. When the load applied in the wear tests is higher ($F_N = 72$ N), the total wear is increased because of the significantly increased wear of the counterspecimen, although the wear of the MMCs is lower than that of the matrix alloy. Therefore, in considering the effect of ceramic particles on the wear resistance of MMCs, one must take the friction couple as a system. The morphology of ceramic particles, their bonding with matrix, the properties of counterspecimen and the load applied will all influence the total wear.

TABLE V Friction coefficient μ of the PM specimens tested against grey cast iron counterspecimen under the reference conditions and at two levels of load ($F_N = 36$ and 72 N)

	Friction coefficient μ	
PM material tested	$F_N = 36$ N	$F_N = 72$ N
At reduction ratio, 5 : 1		
Matrix	0.12	0.35–0.38
Matrix + 10 vol % SiC	0.07	0.28–0.38
Matrix + 10 vol % Al_2O_3	0.10	0.20
At reduction ratio, 20 : 1		
Matrix	0.11	0.20
Matrix + 10 vol % SiC	0.10	0.35–0.39
Matrix + 10 vol % Al_2O_3	0.12	0.27–0.32

The values of friction coefficient μ are presented in Table V. It shows that a much lower friction coefficient was generated when the lower load was applied ($F_N = 36$ N). In this case, μ stabilizes at a level of 0.11–0.12, although the MMCs with SiC and Al_2O_3 reinforcement extruded at 5 : 1 yield even lower μ values, i.e. 0.07 and 0.10, respectively.

When the load applied was low ($F_N = 36$ N), the PM materials extruded at 20 : 1 yielded a friction coefficient at the level of 0.10–0.12. However, at the higher load ($F_N = 72$ N), their friction coefficients moved to a higher level and also showed a much larger scatter in the range from 0.20 to 0.39.

The differences in friction coefficient measured at the different loads may be due to the differences in the freedom of movement of pulled-out hard particles. At $F_N = 36$ N, such particles may well be free to roll between the contacting surfaces, thus lowering friction and, in some cases, also reducing wear due to the formation of three-body abrasion system [15]. At $F_N = 72$ N, however, the pulled-out particles may be pressed into the softer matrix, thus recreating two-body abrasion. That results in higher friction and, in most cases, higher wear. Furthermore, as the friction acts on the specimens in the direction transverse to the extrusion, the structural defects induced during extrusion would act as stress concentration sources. Those located in the subcutaneous layer may easily link up to result in plate-like material removal, as shown in Fig. 8, and thus enhanced wear.

4.4. Tribological tests at 200 °C and in oil

Some encouraging results of the wear tests carried out at room temperature and under the reference conditions, and the requirements of potential users to test the materials under closer-to-real conditions, led to the wear tests at the temperature elevated to 200 °C and in the Shell THERMIA B oil bath. This particular type of oil was chosen because of its high durability at elevated temperatures (up to 380 °C).

The results of the wear tests in the form of volume loss are presented in Fig. 9 and the friction coefficients of the PM specimens are given in Table VI.

TABLE VI Friction coefficient μ of the PM specimens tested against the grey cast iron counterspecimen in the oil bath at 200 °C and at the load of $F_N = 72$ N

PM material tested	Friction coefficient μ $F_N = 72$ N
At reduction ratio, 5 : 1	
Matrix	0.16
Matrix + 10 vol % SiC	0.14
Matrix + 10 vol % Al_2O_3	0.18
At reduction ratio, 20 : 1	
Matrix	0.18
Matrix + 10 vol % SiC	0.16
Matrix + 10 vol % Al_2O_3	0.19

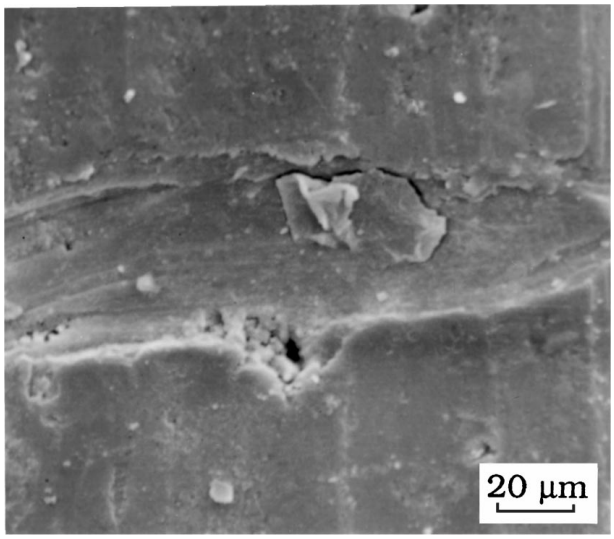

Figure 8 Topography of the composite containing 10 vol % SiC extruded at 20 : 1 and tested at room temperature, at the load of 36 N and in kerosene, after 0.5×10^6 cycles, showing plate-like material removal.

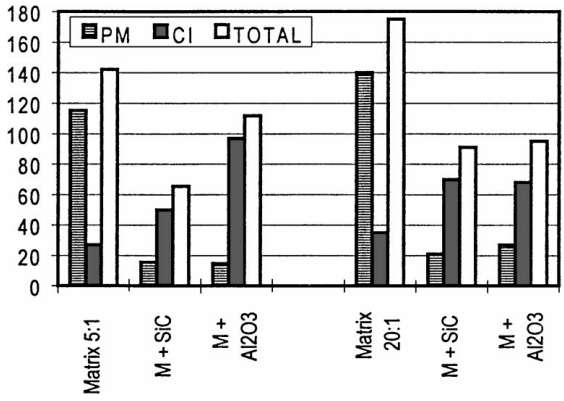

Figure 9 Volume losses per contact cycle V/N_c (mm^3/cycle $\times 10^{-9}$) of the PM specimens and grey cast iron (CI) counterspecimen tested in the Shell THERMIA B oil bath at 200 °C and at the load $F_N = 72$ N.

Over the whole testing time ranging from 30 to 35 h (i.e. $3.5–4 \times 10^6$ cycles), the friction coefficients of the materials remained low. For the PM materials extruded at 5 : 1 and those extruded at 20 : 1, friction coefficient was virtually at the same level, i.e. 0.14–0.18 and 0.16–0.19, respectively. In both cases, the friction force verses time curves were smooth and steady. No signs of sudden collapse of the lubrication layer could be detected. This is in agreement with no vibration of the fretting wear tester or friction-induced noise during the tests. In addition, neither signs of severe wear nor interfacial oxidation process could be observed. After 30–35 h testing, the mating surfaces were only slightly affected by the wear process. They were covered by a hard-to-remove layer, consisting of dense, dark-brown remains of the oil and wear products.

Comparison of the data obtained from the wear tests at the two levels of temperature (see Tables V and VI) shows that testing in the Shell THERMIA B oil at 200 °C instead of in kerosene at room temperature leads to slightly lower μ-values. Clearly, the Shell THERMIA B oil at 200 °C provides better lubrication than kerosene at room temperature.

Again from a practical point of view, the total wear of the friction couple is given in Fig. 9. It is clear that the beneficial effect of ceramic reinforcement in terms of the total wear is indeed obtained under the lubricating conditions at the elevated temperature. One must however note the increased wear of the counterspecimen, which irons out part of the beneficial effect of ceramic reinforcement. This points out the direction of further research, i.e. to change the morphology of ceramic particles in the MMCs for the benefits of the friction couple as a system.

5. Conclusions

1) The processing window for the consolidation of the Al-20Si-5Fe-3Cu-1Mg alloy based composites by hot extrusion is small. The upper temperature limit is imposed by incipient melting of the matrix, while the lower temperature limit is dictated by high deformation resistance of the MMCs. At 450 °C, the MMCs are adhesive to tool-steel die and their matrix may not be ductile enough to withstand the friction. As a result, stick/slip tearing tends to occur when the combination of extrusion parameters is inadequate. This problem should be scrutinized. New die technology applicable to commercial extrusion of the MMCs should be developed.

2) The tensile properties of the MMCs are affected by the value of reduction ratio applied during extrusion. Hot compaction alone is insufficient for complete structural integration from loose powders. A value above 5 : 1 should be used. However, increasing the reduction ratio results in severe structural disturbances of the matrix alloy around SiC or Al_2O_3 particles and the presence of unclosed voids at the longitudinal ends of clustered particles.

3) The wear resistance of the PM materials is also influenced by the value of reduction ratio. This influence is apparent for the PM materials tested in kerosene at room temperature and for those tested in an oil bath at 200 °C. Enhanced wear resistance is obtainable when ceramic reinforcement is firmly embedded in the matrix material. A too high reduction ratio results in decohesion at the interfaces between the matrix and ceramic reinforcement, which leads to delamination and, finally, accelerates the wear of the materials.

4) The addition of ceramic reinforcement to the PM aluminium alloy could increase its wear resistance

considerably. In general, the wear resistance of the MMCs depends on extrusion parameters. For example, the MMCs extruded at 5 : 1 behave better than those extruded at 20 : 1 with respect to mass loss and friction coefficient.

5) Further reduction of wear, both for the MMC specimen and non-MMC counterspecimen, is expected to obtain, when spherical ceramic particles are used for reinforcement, instead of the current angular ceramic particles. Smooth surface of spherical particles will lead to a reduction of the abrasive action of the MMCs on the counterspecimen, in addition to a reduction of the stress concentrations in the MMCs. This should have a positive effect on the total wear of the MMC-containing friction couple.

6) The machining process for the MMCs should be optimized in order to minimize stresses induced. This should also lead to improvement of surface quality and thus enhanced wear resistance of the MMCs.

References

1. A. T. DRUŻDŻEL, Friction and Wear of Al-Based MMCs Under Conditions of Oscillatory Relative Motion, Doctoral Thesis, Delft University of Technology, The Netherlands, 1996.
2. J. ZHOU, J. DUSZCZYK and B. M. KOREVAAR, *J. Mater. Sci*. **26** (1991) 823–834.
3. *Idem., ibid.* **26** (1991) 3041–3050.
4. T. HIRANO, T. OHMI, S. HORI, F. KIYOTO and T. FUJITA, in "Rapidly Solidified Materials," edited by P. W. Lee and R. S. Carbonara (ASM, Metals Park, Ohio, 1986) p. 327.
5. A. T. DRUŻDŻEL, J. ZHOU and J. DUSZCZYK, in Proceedings of 1994 Powder Metallurgy World Congress, Paris, France, 6–9 June 1994 (les Editions de Physique Les Ulis, Paris, 1994) p. 1587.
6. J. E. ALISON and G. S. COLE, *J. Metals* **45**(1) (1993) 19–24.
7. United States Department of Energy—Government Report, December 1990.
8. J. L. ESTRADA and J. DUSZCZYK, *J. Mater. Sci.* **26** (1991) 3909–3213.
9. A. T. DRUŻDŻEL, J. ZHOU, A. W. J. DE GEE, G. J. J. VAN HEIJNINGEN and J. DUSZCZYK, in Proceedings of the 15th Conference on Materials Testing in Metallurgy and 11th Congress on Materials Testing, Balatonszeplak, Hungary, 30 May–1 June 1994, edited by B. Vorsatz and E. Szoke (Hungarian Mining and Metallurgical Society and Scientific Society of Mechanical Engineering, Budapest, 1994) p. 1003.
10. M. J. STARINK, Precipitation Phenomena in Aluminium-Based Metal Matrix Composites: Effect of Reinforcement on Kinetics and Misfit Accommodation, Doctoral Thesis, Delft University of Technology, The Netherlands, 1992.
11. T. S. SRIVASTON, I. A. IBRAHIM, F. A. MOHAMED and E. J. LAVERNIA, *J. Mater. Sci*. **26** (1991) 5965–5978.
12. J. ZHOU, J. DUSZCZYK and B. M. KOREVAAR, in Proceedings of 1990 World Conference on Powder Metallurgy, London, UK, 2–6 July 1990 (The Institute of Metals, London, 1990) Vol. 2, p. 307.
13. GREASLEY and H. Y. SHI, *Powder Metall*. **36** (1993) 288–292.
14. J. ZHOU, A. T. DRUŻDŻEL, J. DUSZCZYK, A. W. J. DE GEE and G. J. J. VAN HEIJNINGEN, in Proceedings of 1994 International Conference on Powder Metallurgy & Particulate Materials, Toronto, Canada, 8–11 May 1994, edited by C. Lall and A. J. Neupaver, (Metal Powder Industries Federation, Princeton, 1994) Vol. 5, p. 339.
15. M. HUTCHINGS, "Tribology: Friction and Wear of Engineering Materials" (Edward Arnold, London, 1992).

Received 17 April 1998
and accepted 23 March 1999